

<https://doi.org/10.1038/s42003-025-07759-9>

One-step Cre-*loxP* organism creation by TAx9



Martin Miguel Casco-Robles¹✉, Tomoki Echigoya², Takeaki Shimazaki³, Yuri Murakami², Masaya Hirano², Fumiaki Maruo¹, Seiya Mizuno¹, Satoru Takahashi^{1,4,5} & Chikafumi Chiba¹✉

The creation of organisms with Cre-*loxP* conditional gene recombination systems often faces challenges, particularly when creating the initial (F0) generation with both a Cre recombinase and a DNA site flanked by *loxP* elements (floxed site). The primary reason is that it is difficult to synthesize a single plasmid with both the Cre gene and the floxed site, since Cre-mediated recombination spontaneously occurs when the plasmid is amplified in *Escherichia coli* bacterial cells. Here, we introduce an artificial nucleic acid sequence TATATATATATATATA, named TAx9, that enables the integration of both the Cre gene and the floxed site into a single plasmid. TAx9 effectively blocks spontaneous Cre-mediated recombination in *E. coli* cells. Using this system, we created an F0 generation of transgenic newts and CRISPR-Cas9 knock-in mice with tissue-specific Cre recombination triggered by tamoxifen. TAx9 technology will be a powerful strategy for creating organisms capable of conditional genetic modification in the F0 generation, accelerating various life science research by reducing the time and cost for ultimately establishing and maintaining lines of genetically modified organisms.

The Cre-*loxP* system is a potent tool that is used in an array of life science fields to address molecular and cellular mechanisms in heredity, development, physiology, disease, and more. Cre is a bacteriophage 38-kDa recombinase that targets a set of 34 bp DNA elements, named *loxP*, and depending on the orientation of the *loxP* sequence, researchers can use it to study deletions, inversions, or the translocation of a DNA site flanked by *loxP* elements (floxed site) in the genomes of organisms^{1,2}. To tactically drive Cre activation in spatial-temporal experiments in eukaryotes, researchers have turned to inducible Cre, such as CreER^{1–4}. In this system, Cre is fused with a modified human estrogen receptor (ER) protein, which is temporarily activated by the administration of a selective estrogen receptor agonist, tamoxifen (or its active metabolite, 4-hydroxytamoxifen (4-OHT)), allowing ER to translocate Cre linked to ER from the cytoplasm to the nucleus across the nuclear envelope in eukaryotes³. Here, CreER expression is also spatially controlled by a tissue-specific promoter³. On the other hand, ER has no role in bacteria, since they are prokaryotes that do not have a nuclear envelope.

It is common practice during the creation of a Cre-*loxP* organism to develop a tissue-specific Cre-driver strain and a *loxP* reporter strain. Both strains can then be bred to obtain a target line. However, in organisms that require a long time to achieve sexual maturation or a generational change,

this poses a great challenge, not only to the cost of their production but also to their maintenance until experimentation. Ideally, plasmids containing both a Cre gene and a floxed site would facilitate the production of genetically modified organisms. However, most attempts to synthesize Cre-*loxP* single plasmids would fail since Cre-mediated recombination occurs in *Escherichia coli* bacterial cells, resulting in the loss of the floxed site from the plasmids^{5,6}. This undesired Cre-mediated recombination in *E. coli* is known to occur not only with Cre and CreER but also with a eukaryotic promoter adjacent to the 5' end of the Cre gene^{5,6}. The possibility that Cre is weakly expressed in *E. coli* has been discussed, although the mechanism is still unclear^{5,6}. In a typical *E. coli* culture for plasmid production, Cre-mediated recombination does not occur in all copies of plasmids. However, this phenomenon is serious from a practical standpoint because it not only reduces the productivity of Cre-*loxP* cells/organisms by transfection/transgenesis but also results in the loss of the Cre-*loxP* single plasmid due to the accumulation of recombined plasmids each time the *E. coli* culture is repeated. To overcome this technical hurdle, CREM, a modified version of Cre, was developed⁵. In this system, the DNA construct encoding Cre contains an altered 5' region and an intron, which does not allow the expression of functional Cre in *E. coli* cells but allows proper Cre expression in mammalian cells, such as CHO-K1 and PC-3 cells⁵. However, since this

¹Institute of Life and Environmental Sciences, University of Tsukuba, Tsukuba, Ibaraki, Japan. ²Graduate School of Science and Technology, University of Tsukuba, Tsukuba, Ibaraki, Japan. ³Graduate School of Life and Environmental Sciences, University of Tsukuba, Tsukuba, Ibaraki, Japan. ⁴Laboratory Animal Resource Center in Transborder Medical Research Center, Institute of Medicine, University of Tsukuba, Tsukuba, Ibaraki, Japan. ⁵Department of Anatomy and Embryology, Institute of Medicine, University of Tsukuba, Tsukuba, Ibaraki, Japan. ✉e-mail: casco.miguel.gm@u.tsukuba.ac.jp; chichiba@biol.tsukuba.ac.jp

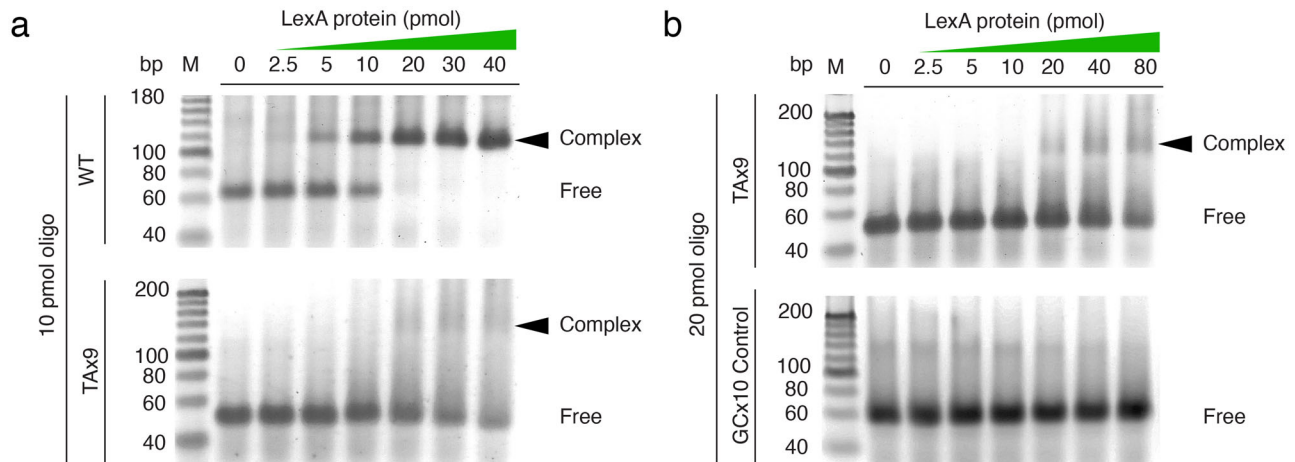


Fig. 2 | The *E. coli* LexA repressor protein binds to the TAx9 element. A gel shift assay was performed to examine the binding affinity of LexA proteins to the TAx9 element in comparison to the LexA binding motif (WT). **a** In the presence of WT oligonucleotides (duplex DNA) at a concentration of 10 pmol, synthetic LexA proteins formed complexes with them at 5 pmol and above. On the other hand, in the presence of 10 pmol of TAx9 oligonucleotides (lower panel), synthetic LexA proteins formed complexes with them at 20 pmol. **b** Increasing the concentration of TAx9 oligonucleotides to 20 pmol resulted in a more distinct band of complexes at 20 pmol

of the synthetic LexA proteins. Note that in both conditions (**a**, **b**), free TAx9 oligonucleotides decreased as the concentration of synthetic LexA protein increased; the data using GCx10 oligonucleotides is shown as a negative control (lower panel in **b**). Taken together, these results indicate that under the current experimental conditions, LexA proteins bind to TAx9 oligonucleotides, although the binding affinity of LexA proteins to TAx9 oligonucleotides is much lower than that to WT oligonucleotides. Black arrowheads indicate the location of complexes.

latter perfectly blocked Cre-mediated recombination or preserved the plasmid's integrity ($n = 6$), even after culturing *E. coli* cells in medium to obtain a sufficient number of plasmids for practical use (Fig. 1c). Thus, we conclude that TAx9 is the minimal element sufficient for Cre-*loxP* single plasmid production.

Since TAx9 suppressed recombination better than WT (i.e., LexA repressor binding motif), we examined in vitro whether the binding affinity of LexA for TAx9 was higher than that for WT. Interestingly, although LexA is bound to TAx9, the binding affinity of LexA for TAx9 was considerably lower than that for WT (Fig. 2).

TAx9 technology enables the creation of Cre-*loxP* animals in the F0 generation

Next, we demonstrate that our TAx9 technology facilitates the creation of Cre-*loxP* organisms. In this study, we attempted to create inducible Cre-*loxP* RPE cell-labeled newts and SMF cell-labeled mice in the F0 generation.

Newts

We applied the above-analyzed plasmid *pmCherry[EGFP]<CAGGs-TAx9-cpRPE65>CreER^{T2}(I-SceI)* (Fig. 3a) to create transgenic *C. pyrrhogaster* newts with the I-SceI technique¹⁰ (Fig. 3b). We obtained a total of 40 individuals that exhibited EGFP+/mCherry- by screening their fluorescence at an early blastula stage (St. 10) and at the larval stage (St. 43) (Fig. 3c), as well as by genomic PCR at the swimming larval stage just before metamorphosis (St. 59) (Fig. 3d). At St. 59, swimming larvae were treated with either 4-OHT or a solvent (DMSO) alone (Fig. 3e). Some of the larvae were subjected to an immunohistochemical analysis (Fig. 4). In the eyeballs, mCherry immunoreactivity was detected along the RPE layer, but not in other ocular tissues, as early as 48 h after 4-OHT administration (Fig. 4a, b). On the other hand, in the control condition with DMSO alone, mCherry immunoreactivity was not detected (Fig. 4a). These results were as expected, with 4-OHT inducing Cre-mediated recombination specifically in RPE cells. The other 4-OHT-treated F0 individuals ($n = 10$) allowed development beyond metamorphosis. All of the larvae grew normally, exceeding one year of age (Fig. 3e).

Mice

We constructed a plasmid *pmCherry[EGFP]<CAGGs-TAx9-hACTA1>CreER^{T2}(ROSA26 Arms)* in *E. coli* cells (Fig. 5a and see Supplementary Fig. 8). Here, the human *ACTA1* promoter (*hACTA1*) was used to specifically drive

expression of the *CreER^{T2}* gene in mouse mature SMF cells⁴. ROSA26 left and right homologous arms^{11,12} were placed at both ends of the transgene cassette to transfer it to the ROSA26 safe harbor site in the mouse genome. Using this plasmid vector, we carried out CRISPR-Cas9 knock-in (KI)¹³ with 283 mouse embryos and obtained 79 neonates (29%) from which 76 individuals (96%) survived beyond the post-weaning period. We examined these individuals by genomic PCR, and finally screened nine individuals (11.8%) that carried the intact transgene cassette in the ROSA26 locus (Fig. 5b–d). In this screening process, PCR bands were never found at either 4.2 kbp for the 5' arm crossing site (Fig. 5c), 1.5 kbp for the floxed site (Fig. 5d), or 6.5 kbp for the full site (Fig. 5d), indicating that undesired Cre-mediated recombination hardly occurs until this stage.

Thus, we successfully obtained Cre-*loxP* mice in the F0 generation. However, more individuals were needed to investigate the induction of SMF cell-specific recombination by tamoxifen. Therefore, we crossed F0 individuals with wild-type mice to obtain F1 individuals. Then, we obtained heterozygous F1 individuals using the same methods that were used for the F0 generation, i.e., screening by fluorescence and genomic PCR. Using these F1 individuals, we tested the effect of tamoxifen administration on SMF cell-specific recombination (Fig. 6 and Supplementary Fig. 9). Genomic PCR analysis revealed that recombination of the floxed site occurred in a tamoxifen dose-dependent manner, with the probability of recombination increasing as the number of doses increased (Fig. 6a). Microscopic analysis of limb tissue sections revealed that mCherry expression was specifically induced in muscle fibers after the administration of tamoxifen (TAM+, $n = 3$; Fig. 6b, c), but not after the administration of the solvent corn oil alone (TAM-, $n = 3$; Fig. 6d, e) (also see Supplementary Fig. 9).

Discussion

The synthesis of Cre-*loxP* single plasmids using *E. coli* bacterial cells has been limited because the *Cre* gene on the plasmid is spontaneously expressed in *E. coli* cells, regardless of the presence of adjacent eukaryotic promoters, and recombination of the floxed site occurs even when using inducible Cre^{5,6}. Therefore, researchers have developed thus far a tissue-specific Cre-driver strain and a *loxP* reporter strain separately and bred them to obtain a target Cre-*loxP* organism. If Cre-*loxP* single plasmids can be synthesized, the efficiency of the development of Cre-*loxP* organisms can be improved in terms of funds, time, space, and other limiting factors,

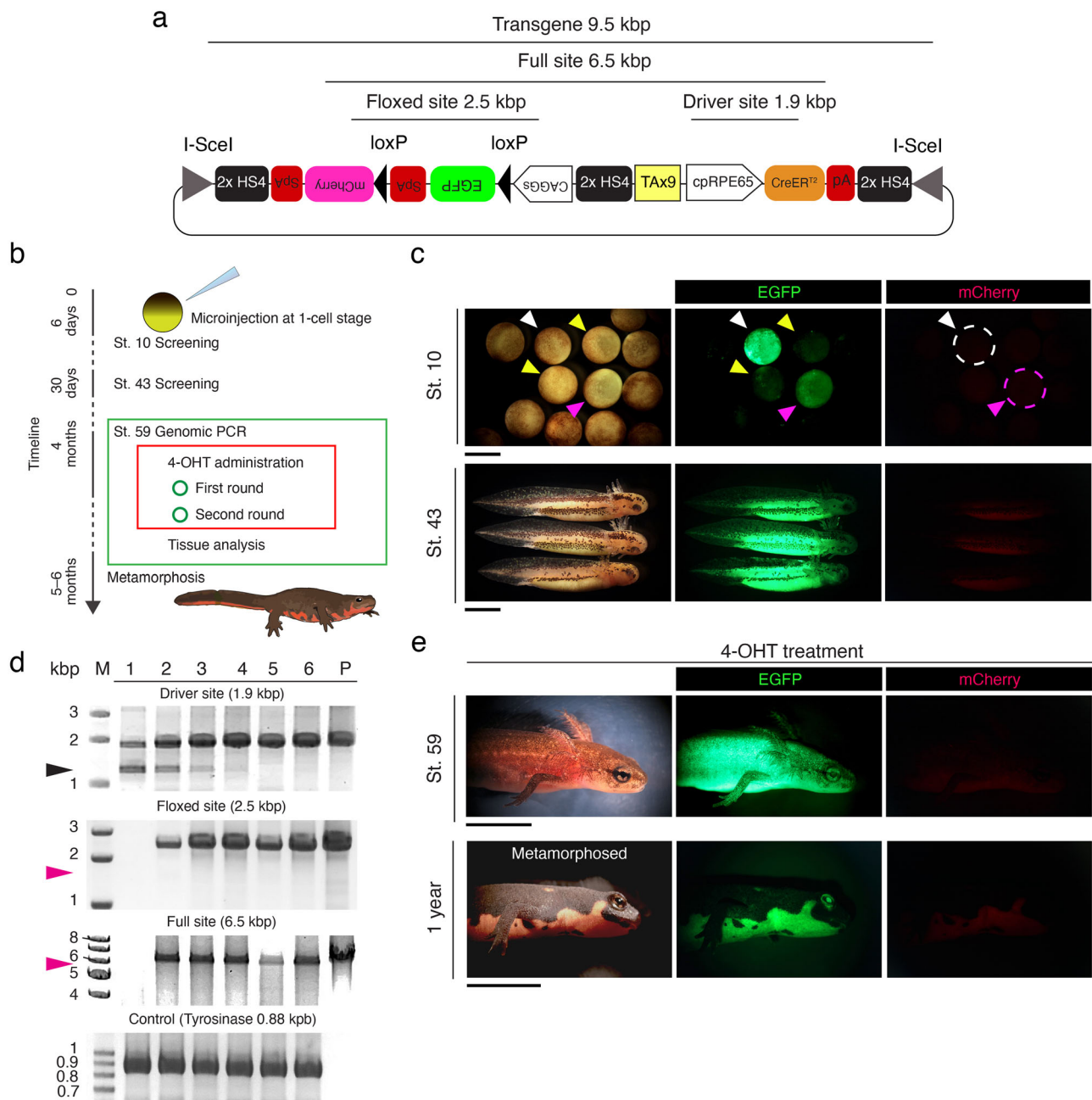


Fig. 3 | TAx9 enables the creation of inducible Cre-loxP RPE cell-labeled newts at F0. a Schematic diagram showing the plasmid *pmCherry[EGFP]<CAGGS-TAx9-cpRPE65>CreER^{T2}(I-SceI)*. **b** Outline of the transgenic protocols. 4-OHT: 4-OH tamoxifen. **c** Screening by fluorescence at an early blastula stage (St. 10) and at the larval stage (St. 43). Individuals never exhibited mCherry fluorescence, and instead emitted EGFP fluorescence. The differential intensity of EGFP fluorescence is thought to be caused by the number of transgene cassettes inserted in the genome, or their location. In St. 10, white, pink, and yellow arrows indicate strong, average, and weak EGFP fluorescence, respectively. Embryos exhibiting strong (white broken circle) or average (pink broken circle) EGFP fluorescence were screened. **d** Screening by genomic PCR at the swimming larval stage (St. 59). Lane numbers indicate the ID of the individual. P: plasmid DNA (control). M: size marker. The full site (6.5 kbp),

driver site (1.9 kbp), and floxed site (2.5 kbp) were examined (see **a**). A 0.88 kbp site of the tyrosinase gene was also examined as the positive control. Black arrowhead: nonspecific band. Pink arrowhead: 1.5 kbp or 5.5 kbp, the size of the band that would be detected if Cre-mediated recombination had occurred. In this group, all larvae were screened as positive, except for the ID#1 individual, whose full and floxed sites were not amplified by PCR. Undesired Cre-mediated recombination was never recognized. **e** Fluorescence after 4-OHT administration. Individuals at St. 59, just before metamorphosis, were treated twice with 4 μ M 4-OHT (see **b**). mCherry fluorescence was never detected, at least not on the surface of the body, at 48 h post-treatment (upper panels) or even beyond metamorphosis (lower panels). All of the metamorphosed individuals ($n = 10$) grew normally, beyond 1 year. Scale bars: **c** 2 mm for St. 10, 2 mm for St. 43; **e** 0.5 cm for St. 59, 1 cm for 1 year.

particularly when studying gene function in animals with long reproductive cycles or small numbers of offspring.

We previously found that a certain genomic region of *X. laevis* (Δ CarA), when present adjacent to the upstream portion of the Cre-driver cassette, suppressed Cre expression in *E. coli* cells, allowing the synthesis of a Cre-loxP single plasmid. Δ CarA contained a region rich in TA/AT repeat

sites, similar to the LexA repressor binding motif (or the SOS box)^{7,8} of *E. coli*. In this study, based on that knowledge, we searched for practical TA/AT repeat elements and demonstrated that TAx9 is an optimal solution. However, it is important to note here that the 115 bp region at the 3' end of Δ CarA, which alone showed a protective effect against Cre-mediated recombination, did not contain TAx9 but instead contained TAx8/ATx8

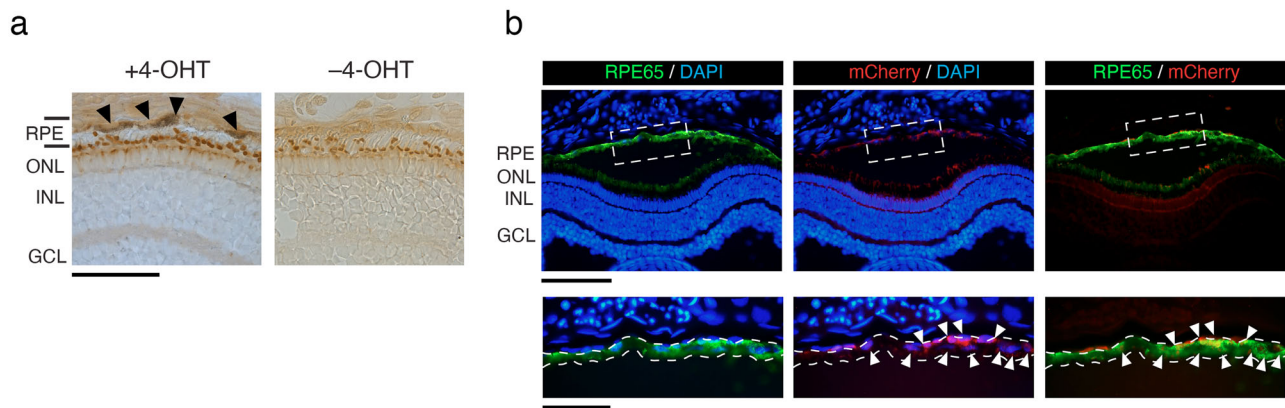


Fig. 4 | 4-OHT induces the expression of mCherry in RPE cells. a Representative images showing 4-OHT-dependent induction of mCherry expression in RPE cells. Larvae at St. 59 were treated with either 4-OHT (+4-OHT) or the solvent (DMSO alone) (−4-OHT) at 48 h before obtaining eyeballs (three larvae for each group). Here, to visualize immunoreactivity in the RPE layer, the ABC-DAB method was applied and melanin pigments were bleached. Arrowheads point to mCherry-immunoreactive cells along the RPE layer. **b** Representative images showing the

double labeling of RPE65 and mCherry in RPE cells by antibodies (three larvae). DAPI: nuclear stain. The lower panels are enlarged views of the area enclosed by the dashed rectangles in the upper panels. In the lower panels, dashed lines highlight the RPE layer. White arrowheads point to the RPE cells with both RPE65- and mCherry-immunoreactivity. GCL: ganglion cell layer; INL: inner nuclear layer; ONL: outer nuclear layer. Scale bars: **a**, 100 μ m; **b**, 200 μ m for upper panels, 100 μ m for lower panels.

(Supplementary Figs. 2 and 7). Since it is unlikely that both TAx8 and ATx8 have a complete shielding effect (Fig. 1b, c), it is possible that adjacent DNA structures of TAx8/ATx8 in Δ CarA have some complementary effect.

Regarding TAx9, since a synthetic LexA repressor protein can bind to TAx9 duplex DNA (Fig. 2), it is thought that Cre expression in *E. coli* cells is suppressed by LexA repressor binding to TAx9, which inhibits the activity of the adjacent promoter. However, importantly, the binding affinity of LexA repressor for TAx9 was considerably lower than for the LexA repressor binding motif (Fig. 2a), although the inhibitory effect of TAx9 on Cre-mediated recombination was higher and more complete than that of the LexA repressor binding motif (Fig. 1). In the future, it will be necessary to investigate the possibility that the interaction between LexA and TAx9 (or between LexA and the LexA binding motif) is altered in *E. coli* cells, as opposed to in vitro. An alternative explanation may lie in the structural nature of the AT/TA sequences. Studies have found that the dodecamer d(ATATATATATAT) sequences form very stable coiled coils^{14,15}. This coiling nature of AT/TA, when positioned upstream of a promoter, may act as a coiled barrier that prevents the transcription of Cre¹⁶. However, this mechanism cannot explain why other AT/TA elements, such as ATx9 or TAx10, had no barrier effects (Fig. 1b).

Using the TAx9 technology, we synthesized single Cre-*loxP* plasmids in *E. coli* cells, and succeeded in creating inducible Cre-*loxP* transgenic newts (RPE cell-labeled) and CRISPR-Cas9 KI mice (SMF cell-labeled) in the F0 generation. In both animals, TAx9 did not affect normal development and growth. In addition, Cre-mediated recombination in the target cell type was induced by treatment with 4-OHT or tamoxifen, indicating that there is no spontaneous recombination at the floxed site and, unlike in *E. coli* cells, TAx9 does not seriously affect the activity of the Cre-driver cassette. For newts, F0 individuals could be used directly in retinal regeneration studies by carefully evaluating the specificity of the expression regions. For mice, however, although F0 individuals were obtained in this study, recombination was evaluated in F1 individuals due to a limited number of individuals. In KI mice, researchers generally perform multiple backcrosses with wild-type mice to eliminate the possibility that transgene constructs have been randomly inserted into non-target regions of the genome, thereby establishing a strain. Under these circumstances, our technology will contribute to the ability to efficiently establish mouse lineages (Supplementary Fig. 10). If the Cre and *loxP* cassettes are separate, mating could cause each cassette to segregate into different offspring, but if a single plasmid is used to create KI mice, the Cre-*loxP* cassette can be maintained at a single locus, avoiding this problem. Moreover, the fact that the Cre-*loxP* cassette is at a single locus facilitates strain maintenance with a single genotyping protocol.

In principle, TAx9 technology can be applied not only to standard and inducible Cre-*loxP* systems but also to a variety of conditional gene modification tools such as Flp-*frt*^{17,18} and Dre-*rox*^{18,19}. These technologies can be combined with RNA interference²⁰ or CRISPR-Cas9 genome editing tools²¹, thereby enabling not only forced gene expression but also gene knockdown/knockout in spatially and temporally restricted ways. Moreover, TAx9 technology is versatile because it is likely independent of animal species and cell types. Of course, more research is needed to demonstrate that TAx9 does not have any effect on any type of promoter or on the expression of any recombinase gene in any animal (or any organism) or cell type. Through these validations, TAx9 technology will contribute to various fields of life science in the future.

Methods

All experiments reported herein were performed at the University of Tsukuba, in accordance with its guidelines and regulations. All protocols with animals were approved by the Animal Care and Use Committee of the University of Tsukuba (approval numbers: for newts, 170110 and 220125; for mice, 23–310 and 24–167). All genetic modification experiments were approved by the Genetic Modification Safety Committee of the University of Tsukuba (approval numbers: 170110, 220124, and 220125). Moreover, all methods were reported in compliance with the ARRIVE guidelines 2.0²².

Animals

We have complied with all relevant ethical regulations for animal use.

Adult *C. pyrrhogaster* newts (total body length: males, ~9 cm; females, 11–12 cm) of the Toride-Imori line²³ were used to obtain fertilized eggs for transgenesis. They were originally captured by a provider (Mr. Kazuo Ohuchi, Misato, Saitama, 341-0037 Japan; <http://kaeru-kerokero.la.coocan.jp/index.html>) within a ~25 km diameter around the Miyayama area (35.130013, 140.013842) in Kamogawa city, Chiba prefecture, Japan. No specific permissions were required for the location of capture. Newts were reared for longer than one year in the laboratory (University of Tsukuba) by keeping them in plastic containers in which a shallow layer of water (~3 cm deep) and a resting island were placed, at 18°C and in natural light, as was previously described²⁴. In this study, 30 females and 10 males were kept in separate containers for 60 days until the transgenic experiments began. Both of them were fed frozen mosquito larvae (Akamushi; Kyorin Co., Ltd., Hyogo, Japan) three times a week. Containers were kept clean. To obtain fertilized eggs at the 1-cell stage (F0), adult newts were maintained according to a previously established protocol¹⁰. Using fertilized eggs ($n = 84$), transgenesis was carried out (see below), and embryos and larvae were staged

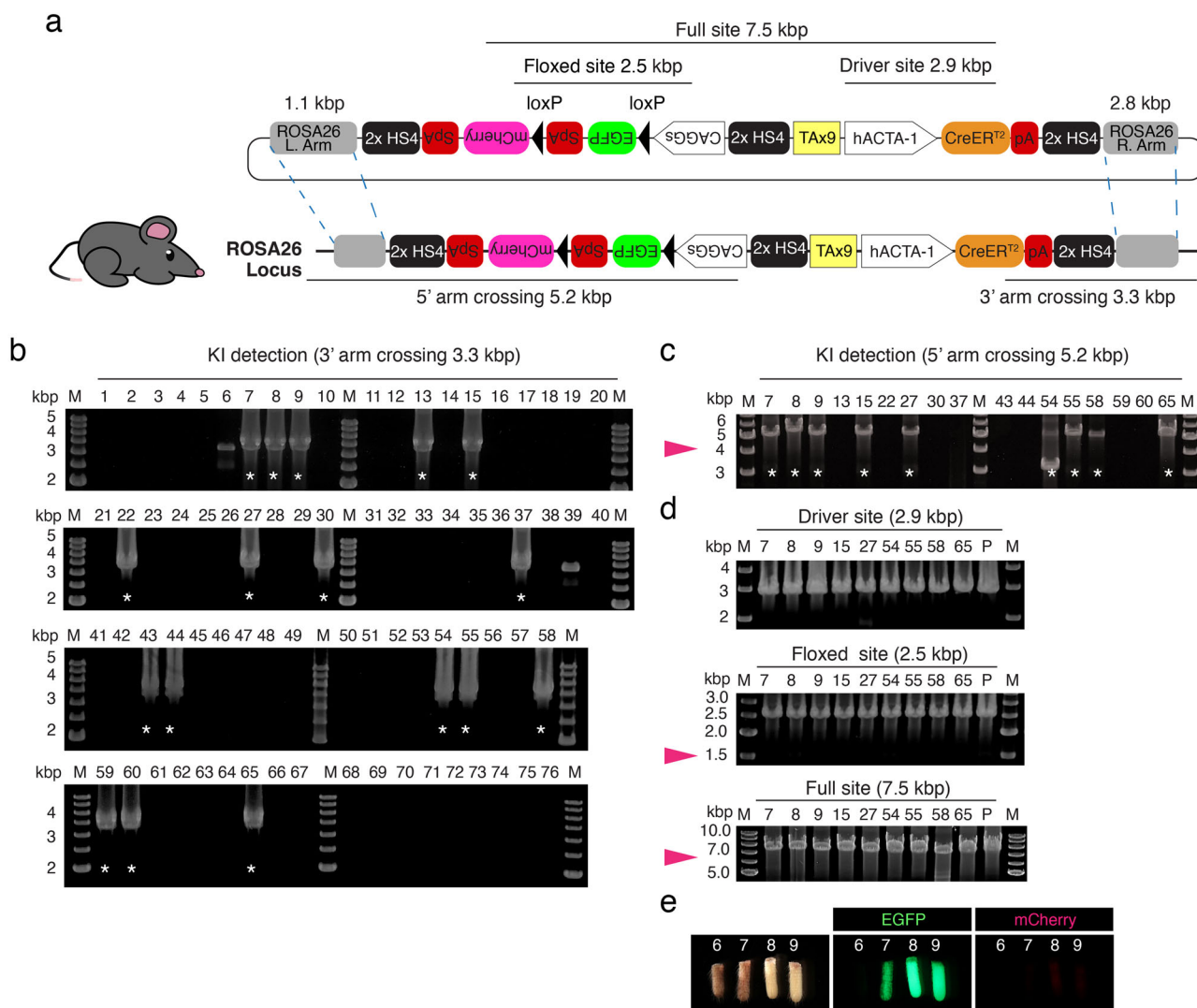


Fig. 5 | *TAx9* enables the creation of inducible *Cre-loxP* SMF cell-labeled mice at F0. **a** Schematic diagram showing the plasmid *pmCherry/EGFP*<*CAGGS-TAx9-hACTA1*>*CreER^{T2}*(*ROSA26 Arms*) designed to create SMF cell-labeled mice by the CRISPR-Cas9 knock-in (KI) protocol targeting the *ROSA26* locus^{11,12} (also see Supplementary Fig. 8). The sites amplified by genomic PCR are noted. **b–d** Screening of KI individuals by genomic PCR. Here, a total of 76 one-month-old individuals who survived beyond the weaning period were examined. Lane numbers indicate the ID of the individual. P: plasmid DNA (control). M: size marker. The first PCR for the 3' arm crossing site (3.3 kbp) (**b**) followed by the second PCR for the 5' arm crossing site (5.2 kbp) (**c**) screened nine individuals as positive candidates (white asterisks).

Individuals with ID#s 13, 22, 30, 37, 43, 44, 59, and 60 are considered to be individuals with DNA fragments containing the 3' arm crossing site but not the 5' arm crossing site, that were inserted randomly into the genome. KI of the single *Cre-loxP* construct in all these candidates was confirmed by the last PCR for the driver site (2.9 kbp), the floxed site (2.5 kbp), and the full site (7.5 kbp) (**d**). **e** Fluorescence of the tail tip of KI-positive (#7, #8, #9) and KI-negative (#6) individuals. All of the KI-positive individuals showed EGFP fluorescence but not mCherry fluorescence, indicating that Cre-mediated recombination had not occurred. Pink arrowhead: 4.2 kbp (c), 1.5 kbp (d), or 6.5 kbp (d), indicating the size of the band that would be detected if Cre-mediated recombination had occurred. Scale bar: 5 mm.

according to established criteria²⁴. A total of 10 transgenic individuals were finally screened and their recombination was examined without distinguishing between sexes (see the “Induction of Cre-mediated recombination” section).

Adult C57BL/6J mice (Strain #: 000664; RRID: IMSR JAX:000664) were purchased from Jackson Laboratory Japan Inc. (Kanagawa, Japan)¹¹ and kept in the Laboratory Animal Resource Center in the Transborder Medical Research Center. They were housed with a 14-h light: 10-h dark cycle. Air quality was maintained under specific pathogen-free conditions (23.5 °C ± 2.5 °C and 52.5% ± 12.5% relative humidity)¹¹. They were fed a commercial diet (MF diet; Oriental Yeast Co., Ltd., Tokyo, Japan) and could drink filtered water, both of which were freely accessible. For CRISPR-Cas9 KI, a total of 283 embryos were used, a total of 76 individuals (males: 39; females: 37) survived beyond the post-weaning period, and a total of nine individuals (males: two; females: seven) were finally screened as F0. For

experiments with F1 to F4, a total of 117 individuals (males: 57; females: 60) were used. In the recombination experiments in Fig. 6, three males and three females were used for the test (for 3D, one male, two females; for 6D, two males, one female) while one male and two females were used for the control (TAM−) (see the “Induction of Cre-mediated recombination” section).

Only skilled researchers handled both the newts and mice. There were no unexpected adverse events.

Plasmid construction

All plasmids used herein were constructed and synthesized by standard molecular cloning techniques. In brief, to screen for optimal DNA elements to protect *Cre-loxP* single plasmids from Cre-mediated recombination in *E. coli* cells, a region containing *CarA*>*CreER^{T2}* was removed from the plasmid *pmCherry/EGFP*<*CAGGS-CarA*>*CreER^{T2}* (*I-SceI*)²⁵ with the restriction enzymes, *BspEI* and *AjuI*, and then a fragment *BspEI*-*PpuMI*-*I-PpoI*>*CreER^{T2}*

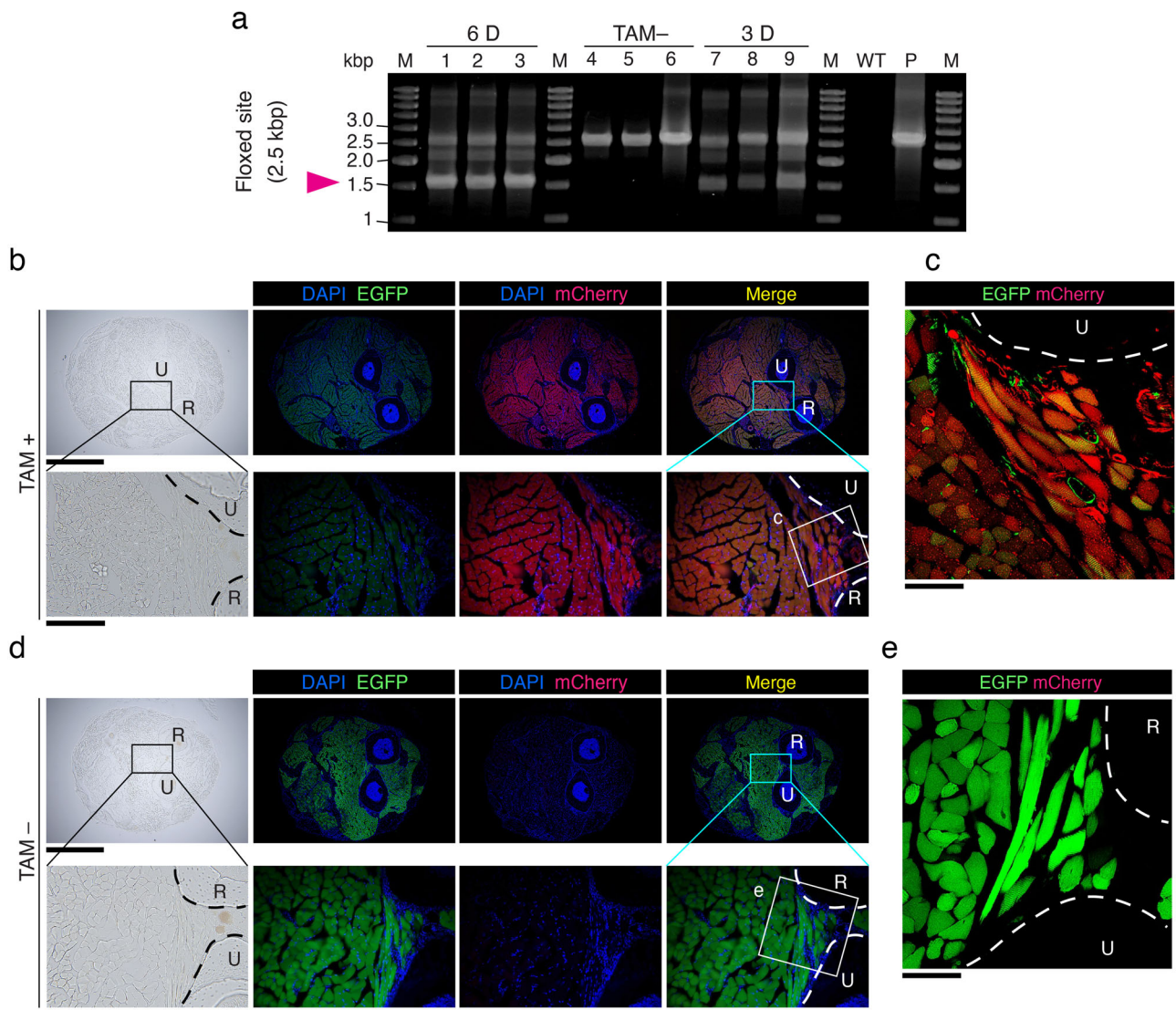


Fig. 6 | Tamoxifen induced the expression of mCherry in SMF cells. **a** Genomic PCR for the floxed site in F1 heterozygous KI mice (intact, 2.5 kbp; recombined, 1.5 kbp). These mice were injected with three doses (3D) or six doses (6D) of tamoxifen or the solvent corn oil alone (TAM–) two weeks before limb sample collection ($n = 3$ each). Lane numbers indicate the ID of the individual. WT: genomic DNA of a wild-type C57BL/6J mouse. P: plasmid DNA (control). M: size marker. Pink arrowheads: 1.5 kbp (recombined). **b–e** Representative images showing tamoxifen-dependent induction of mCherry expression in SMF cells ($n = 3$ for each). F1 heterozygous KI mice were injected with either six doses of tamoxifen (TAM+) or

the solvent corn oil alone (TAM–). The limb samples were cross-sectioned in the middle of the zeugopod (20 μm thick). mCherry fluorescence was detected in the TAM+ mice (**b, c**) but not in the TAM– mice (**d, e**). Note that EGFP fluorescence in the TAM+ mice was weaker than in the TAM– mice, suggesting recombination of the floxed site. The optical sections (1.3–2.0 μm thick) of the boxed areas of the merged images in (**b**) and (**d**), acquired by laser confocal microscopy, are shown in (**c**) and (**e**), respectively. Scale bars: **b** and **d** 1 mm for upper panels, 200 μm for lower panel; **c** and **e** 100 μm .

was inserted back in, creating a new intermediate plasmid *pmCherry[EGFP]<CAGGs-BspEI-PpuMI-I-PpoI>CreER^{T2} (I-SceI)*. The I-PpoI restriction enzyme recognition site was used to insert a promoter to drive the expression of *CreER^{T2}*. In this study, a 1.1 kbp fragment containing the *cpRPE65* promoter and its 5' UTR region⁹ were inserted. The *BspEI-PpuMI* site was referred to as TA(ID), which was used to insert a candidate protective DNA element indicated in Fig. 1a.

To create inducible *Cre-loxP* RPE cell-labeled newts, the plasmid *pmCherry[EGFP]<CAGGs-TAx9-cpRPE65>CreER^{T2} (I-SceI)* was constructed (Fig. 3a). Here, *TAx9* was inserted at the TA(ID) site. The transgene cassette was flanked by the I-SceI meganuclease recognition sites. The chicken β -globin HS4 2 \times core insulators (a gift from Dr. Gary Felsenfeld at the National Institute of Health, Bethesda, MD, USA) were placed at both ends of the *Cre-driver* cassette and the floxed reporter cassette to reduce the positional genomic effects and *cis* interactions

within the transgene. Each of the *EGFP*, *mCherry*, and *CreER^{T2}* gene cassettes was followed by an eukaryotic terminal polyadenylation signal sequence (for details, see Fig. 1).

To create inducible *Cre-loxP* SMF cell-labeled mice, the plasmid *pmCherry[EGFP]<CAGGs-TAx9-hACTA1>CreER^{T2}(ROSA26 Arms)* was constructed (Fig. 5a and see Supplementary Fig. 8). At first, the human *ACTA1* skeletal muscle promoter⁴ fragment (–1919 to +156 in exon 1) was inserted at the I-PpoI site in the plasmid *pmCherry[EGFP]<CAGGs-TAx9-I-PpoI>CreER^{T2} (I-SceI)*, creating the plasmid *pmCherry[EGFP]<CAGGs-TAx9-hACTA1>CreER^{T2} (I-SceI)*. Next, the entire transgene cassette was released by I-SceI digestion and inserted into a *ROSA26* targeting vector^{11,12}, so that the transgene cassette had the homologous arms targeting the *ROSA26* locus adjacent to both ends of the cassette (1.1 kbp at the 5' side and 2.8 kbp at the 3' side)^{11,12}. This cassette also contained three sets of the chicken β -globin HS4 2 \times core insulators.

For all plasmids, *E. coli* cells of the NEB stable strain (C3040I; New England Biolabs, Ipswich, MA, USA) were transformed and cultured on LB plates at 30°C for 18 h. Colonies on the plates were individually examined by PCR for Cre-mediated recombination in plasmids, and cultured in LB medium for an additional 18 h at 30°C. The plasmids synthesized in the *E. coli* cell culture were purified using the GeneJET Plasmid Miniprep Kit (K0502; Thermo Fisher Scientific Inc., Tokyo, Japan) or the PureLink HiPure Plasmid Filter Midiprep Kit (K210014, Invitrogen; Thermo Fisher Scientific Inc.) according to the manufacturer's instructions.

Exceptionally, as explained in the "Attaining the TA repeat sequences" section of the Supplementary Information, insert DNA was obtained by PCR and ligated into plasmids using the In-Fusion method (Z9649N; In-Fusion® HD Cloning Kit, Takara Bio Inc., Shiga, Japan) according to the manufacturer's instructions. *E. coli* cells used for transformation and culture were the Stbl3 strain (One Shot™ Stbl3™ Chemically Competent *E. coli*; C737303, Invitrogen, Thermo Fisher Scientific Inc.). The culture conditions were the same as those for the NEB stable strain mentioned above. As shown in Supplementary Fig. 7, inserts containing TA/AT-rich sites were amplified using Tks Gflex DNA Polymerase (R060A; Takara Bio Inc.) according to the manufacturer's instructions. In the experiments to evaluate *Cre* gene expression in *E. coli* cells (Supplementary Fig. 5), total RNA was purified using the SV Total RNA Isolation System (Z3100; Promega, Madison, WI, USA) and amplified using the One Step RNA PCR Kit (AMV) (RR024A; Takara Bio Inc.) according to the manufacturer's instructions.

Gene modification

For transgenic newts, an I-SceI protocol we established for *C. pyrrhogaster*¹⁰ was applied. Briefly, fertilized eggs (one-cell stage embryos) were individually micro-injected with 100 pg of plasmid DNA and 2.0×10^{-3} U of I-SceI, which were dissolved in $1 \times$ I-SceI buffer. For CRISPR-Cas9 KI mice, a protocol we established^{11–13} was applied with a guide RNA targeting 5'-CCAGTCTTTCTAGAAGATGGGCG-3' in the ROSA26 locus (chr6: qE3). Preparation of crRNA, tracrRNA, Cas9, and donor DNA, micro-injection into mouse zygotes, and embryo transfer into pseudopregnant mice were all performed using the same methods as in our previous papers^{11–13}.

Anesthesia

Larval newts (St. 59) were anesthetized with FA100 (4-allyl-2-methoxyphenol; DS Pharma Animal Health, Osaka, Japan) dissolved to 0.05% (v/v) in filtered tap water at 18 °C; for image capture, 30 min; for tail tip sampling, 30 min; for head collection or euthanasia for culling, deep anesthesia as long as 60 min (the larvae remain in an upside down position and do not respond to cutaneous pinching with forceps) followed by decapitation. Mice were anesthetized by intraperitoneal injection of a mixture of ketamine and xylazine; for tail tip sampling, 80 mg/kg ketamine and 10 mg/kg xylazine (10 min); for forelimb collection or euthanasia for culling, an overdose of the anesthetics (triple the dosage; 15–20 min) followed by cervical dislocation. In both conditions, we confirmed that the mice were unresponsive to pinching of their legs and tails.

Genomic PCR

Genomic DNA was obtained from the tail tips of larval newts (St. 59) and mice (1 month old) with a Wizard Genomic DNA Purification Kit (A1120; Promega). For mice, limb muscles were also used (see below). The genomic DNA solution was aliquoted to 10 ng/μL and kept at 4 °C. PCR was carried out using Tks Gflex DNA Polymerase (R060A; Takara Bio Inc.) according to the manufacturer's instructions. Primer sets are listed in Supplementary Table 1.

Induction of Cre-mediated recombination

For larval newts (St. 59), the method we established²⁶ was applied. In brief, larvae were incubated in filtered tap water containing 4 μM 4-OHT ((Z)-4-hydroxytamoxifen, H7904-5MG; Sigma-Aldrich; Merck, Darmstadt, Germany) and 0.8% (v/v) dimethylsulfoxide (DMSO; 045-07216; FUJIFILM Wako Pure Chemical Corporation, Osaka, Japan) for 24 h at 22 °C in the

dark (first round). They were immediately transferred into fresh 4-OHT-containing water and incubated for an additional 24 h in the same conditions (second round). For control, larvae were incubated in filtered tap water containing DMSO alone.

For mice (1 month old), a standard peritoneal injection protocol was applied. In brief, tamoxifen (T5648-1G, Sigma-Aldrich; Merck) was dissolved in corn oil (032-17016, Wako Pure Chemical Corporation) at a concentration of 20 mg/mL for 1 h at 65 °C in the dark and vortexed, and the liquid was divided into 1 mL aliquots and stored at 4 °C (it was used within 1 week). Just before injections, aliquots were prewarmed for 10 min at 65 °C, cooled to room temperature, and then injected with a 27-gauge needle (NN-2719S; Terumo, Tokyo, Japan) to achieve 150 mg/kg body weight. Injections were given once a day for three consecutive days, followed by a four-day interval, and then again for three consecutive days (six doses in total). Following the last injection, mice were allowed to rest for 2 weeks. For the control, corn oil alone was injected.

Tissue preparation

In this study, a fixative, 3% glyoxal^{27,28} (078-00905, FUJIFILM Wako Pure Chemical Corporation) and 2% paraformaldehyde (PFA; Catalog 26126-25; Nacalai Tesque, Inc., Kyoto, Japan) in phosphate-buffered saline (PBS; pH 7.0, adjusted with acetic acid) was prepared, stored in an amber-colored glass bottle at 4 °C, and used within 1 month.

Heads of larval newts (St. 59) were collected in PBS on ice, and immediately transferred into the fixative and incubated at 4 °C for 8 h. The samples were washed several times for 3 h each in PBS at 4 °C, decalcified in 10% ethylenediamine-N,N,N',N'-tetraacetic acid (EDTA) in PBS (pH 7.0, adjusted with NaOH) for 48 h at 4 °C, rinsed in PBS, and then transferred to 30% sucrose in PBS at 4 °C.

Forelimbs of mice (1 month old) were collected in PBS on ice following cervical dislocation, their skin was removed, and they were trimmed to obtain a portion from the wrist to the distal end of the humerus. Limb muscles for genomic DNA were sampled at this time. The deskinning forelimb samples were immediately fixed at 4 °C for 18 h, washed several times for 3 h each in PBS at 4 °C, and incubated in a decalcifying solution (10% EDTA in PBS (pH 7.0, adjusted with NaOH)) for 72 h at 4 °C, rinsed in PBS, and then transferred to 30% sucrose in PBS at 4 °C.

Following the equilibration process in sucrose solution, newt head and mouse forelimb samples were embedded into an O.C.T compound (45833; Sakura Finetech, Tokyo, Japan) and sectioned to 20 μm thickness using a cryotome (CM1860 UV, Leica Biosystems, Tokyo, Japan). Frozen sections were air dried in the dark for 24 h before proceeding to the direct observation of their fluorescence or immunohistochemistry.

Immunohistochemistry

Primary antibodies were mouse monoclonal anti-RPE65 antibody (1:500; MAB5428; EMD Millipore, Burlington, CA, USA), and rabbit polyclonal anti-RFP antibody (for mCherry; 1:500; 600-401-379; Rockland Immunochemicals, Pottstown, PA, USA). Secondary antibodies were Alexa 488-conjugated goat anti-mouse IgG (H+L) antibody (1:500; A11001; Thermo Fisher Scientific Inc.); rhodamine (TRITC)-conjugated affiniPure goat anti-rabbit IgG (H+L) antibody (1:500; Code: 111-025-003; Jackson ImmunoResearch Laboratories, West Grove, PA, USA), and biotinylated goat anti-rabbit IgG (1:250; BA-1000; Vector Laboratories, Inc., Newark, CA, USA). Immunohistochemistry was performed as in a previous paper²⁶, with some modifications. In brief, for immunofluorescence labeling, tissue sections were washed (PBS, 15 min; 0.1% Triton X-100 in PBS, 15 min; and PBS, 15 min), incubated with blocking solution (2% normal goat serum (S-1000; Vector Laboratories), 50% animal free blocker (SP-5035-100, Vector Laboratories) and 0.1% Triton X-100 in PBS) for 2 h, and then incubated with primary antibody diluted in blocking solution overnight at 4 °C. The sections were washed and then incubated with a secondary antibody diluted in a blocking solution for 4 h. After washing, the sections were counterstained with 4,6-diaminodino-2-phenylindole (DAPI, 1: 50,000; D1306; Thermo Fisher Scientific Inc.).

For immunoperoxidase labeling, tissue sections were washed, and incubated in a blocking solution mixed with Avidin D (1:50; Avidin/Biotin Blocking kit; SP-2001; Vector Laboratories Inc.) for 2 h, washed with PBS, then incubated in primary antibody diluted with blocking solution containing biotin (1:50; Avidin/Biotin Blocking kit) overnight at 4 °C. The sections were washed, incubated with biotinylated secondary antibody in blocking solution for 4 h, washed, incubated with 0.1% Triton X-100 in PBS containing avidin and biotin complex (1:50 each; Vectastain ABC Elite kit; PK-6100; Vector Laboratories Inc.) for 2 h, washed, then treated with 3,3'-diaminobenzidine (DAB) solution (DAB substrate kit; SK-4100; Vector Laboratories Inc.). Following labeling, the sections were washed and counterstained with DAPI. For ocular sections of newt larvae, melanin pigments of the RPE layer were bleached with PBS containing 3% H₂O₂ and 1.5% sodium azide²⁶.

Gel shift assay

The WT (LexA binding element), TAx9, and GCx10 (negative control) containing single-strand oligonucleotides were self-annealed using conventional molecular cloning techniques to form duplex DNAs. In brief, the forward and reverse single-strand oligos of equal concentration (Supplementary Table 2) were heated at 95 °C for 3 min, incubated at 85 °C for 1 min, and then subjected to the same treatment until a total of 60 steps, where the annealing temperature was lowered by 1 °C in each successive step. Complexes of the *E. coli* LexA recombinant protein (01-005; Cosmo Bio, Tokyo, Japan) with each duplex DNA were formed according to established optimized methods for the WT (i.e., the SOS box) duplex DNA⁷. The protein-DNA reaction products (10 µL) were electrophoresed on 3.2% agarose gels (Agarose 21; 313-03242; Nippon Gene, Tokyo, Japan) in 0.5x TBE (45 mM Tris-borate, 1 mM EDTA) buffer at 4 °C and 100 V for 70 min.

Statistics and reproducibility

For *E. coli*, mice, and newts, at least three samples (experimental unit: a bacterial colony or a single animal) were analyzed per examination. No statistical comparisons of means or variances among multiple groups were made in this study. No data were excluded from the analyses. A minimum of three biological replicates were used in each evaluation since we employed only already established techniques in this study. In the case of recombination experiments, CreER^{T2}-loxP animals were randomly separated into two groups before tamoxifen (test group) or DMSO/corn oil (control group) administration. There was no need for blind grouping because CreER^{T2}-loxP animals with similar EGFP fluorescence were used. Data were evaluated independently by several authors. Potential confounders were not considered.

Microscopy and image analysis

Fluorescence of living newts and tail tips of mice were observed under a fluorescence dissecting microscope (M165 FC; Leica Microsystems, Tokyo, Japan) equipped with filter sets for EGFP (Leica GFP-Plant; exciter: 470/40 nm; emitter: 525/50 nm) and mCherry (exciter: XF1044, 575DF25; emitter: XF3402, 645OM75; Opto Science, Tokyo, Japan), which were designed to minimize bleed-through artifacts. Images were captured with a digital camera system (EOS Kiss x7i; Canon, Tokyo, Japan) attached to the microscope. Tissue sections were observed on a fluorescence microscope (BX50; Olympus, Tokyo, Japan) equipped with the same filter sets for EGFP and mCherry as well as that for DAPI. Images were captured with a charge-coupled device camera system (DP73; cellSens Standard 1.6; Olympus) attached to the BX50 microscope. For mouse limb sections, a laser confocal microscope system (LSM700; ZEN 2009, ver. 6.0.0.303; Carl Zeiss, Oberkochen, Germany) with filter sets for EGFP (Diode 488 Laser; emitter: BP 515–565 nm) and mCherry (Diode 555 Laser; emitter: BP 575–640 nm) was used. Images were analyzed with the software of the image acquisition systems and the functions of Adobe Photoshop 25.11.0 (Adobe, San Jose, CA, USA). The brightness, contrast, and sharpness of images were adjusted according to the journal's guidelines using Photoshop 25.11.0. All gel

electrophoresis data employed in this study are images of a single uncut gel containing size markers (for raw data, see Supplementary Fig. 11). Some images were inverted (Figs. 1–3 and Supplementary Fig. 5). Panels and Figures were prepared using Illustrator 27.4.1 graphics software (Adobe).

Reporting summary

Further information on research design is available in the Nature Portfolio Reporting Summary linked to this article.

Data availability

The data that support the findings of this study are available from the corresponding authors upon reasonable request.

Received: 11 September 2024; Accepted: 17 February 2025;

Published online: 06 March 2025

References

- Kim, H., Kim, M., Im, S.-K. & Fang, S. Mouse Cre-LoxP system: general principles to determine tissue-specific roles of target genes. *Lab. Anim. Res.* **34**, 147 (2018).
- Brocard, J. et al. Spatio-temporally controlled site-specific somatic mutagenesis in the mouse. *Proc. Natl Acad. Sci. USA* **94**, 14559–14563 (1997).
- Feil, R., Wagner, J., Metzger, D. & Chambon, P. Regulation of Cre recombinase activity by mutated estrogen receptor ligand-binding domains. *Biochem. Biophys. Res. Commun.* **237**, 752–757 (1997).
- McCarthy, J. J., Srikuea, R., Kirby, T. J., Peterson, C. A. & Esser, K. A. Inducible Cre transgenic mouse strain for skeletal muscle-specific gene targeting. *Skelet. Muscle* **2**, 8 (2012).
- Kaczmarczyk, S. J. & Green, J. E. A single vector containing modified cre recombinase and LOX recombination sequences for inducible tissue-specific amplification of gene expression. *Nucleic Acids Res.* **29**, 56e–556e (2001).
- Fernández-Chacón, M. et al. iSuRe-Cre is a genetic tool to reliably induce and report Cre-dependent genetic modifications. *Nat. Commun.* **10**, 2262 (2019).
- Zhang, A. P. P., Pigli, Y. Z. & Rice, P. A. Structure of the LexA–DNA complex and implications for SOS box measurement. *Nature* **466**, 883–886 (2010).
- Culyba, M. J., Kubiak, J. M., Mo, C. Y., Goulian, M. & Kohli, R. M. Non-equilibrium repressor binding kinetics link DNA damage dose to transcriptional timing within the SOS gene network. *PLoS Genet.* **14**, e1007405 (2018).
- Casco-Robles, M. M., Miura, T. & Chiba, C. The newt (*Cynops pyrrhogaster*) RPE65 promoter: molecular cloning, characterization and functional analysis. *Transgenic Res.* **24**, 463–473 (2015).
- Casco-Robles, M. M. et al. Expressing exogenous genes in newts by transgenesis. *Nat. Protoc.* **6**, 600–608 (2011).
- Hasegawa, Y. et al. Novel ROSA26 Cre-reporter knock-in C57BL/6N mice exhibiting green emission before and red emission after Cre-mediated recombination. *Exp. Anim.* **62**, 295–304 (2013).
- Nakashiba, T. et al. Development of two mouse strains conditionally expressing bright luciferases with distinct emission spectra as new tools for in vivo imaging. *Lab Anim.* **52**, 247–257 (2023).
- Tanimoto, Y. et al. Zygote microinjection for creating gene cassette knock-in and flox alleles in mice. *J. Vis. Exp.* **184**, e64161 (2022).
- Campos, J. L., Urpí, L., Sanmartín, T., Gouyette, C. & Subirana, J. A. DNA coiled coils. *Proc. Natl Acad. Sci. USA* **102**, 3663–3666 (2005).
- Valls, N., Richter, M. & Subirana, J. A. Structure of a DNA duplex with all-AT base pairs. *Acta Crystallogr. D Biol. Crystallogr.* **61**, 1587–1593 (2005).
- Dorman, C. J. DNA supercoiling and transcription in bacteria: a two-way street. *BMC Mol. Cell Biol.* **20**, 26 (2019).
- Yamamoto, M. et al. A multifunctional reporter mouse line for Cre- and FLP-dependent lineage analysis. *Genesis* **47**, 107–114 (2009).

18. Karimova, M. et al. A single reporter mouse line for Vika, Flp, Dre, and Cre-recombination. *Sci. Rep.* **8**, 14453 (2018).
19. Anastassiadis, K. et al. Dre recombinase, like Cre, is a highly efficient site-specific recombinase in *E. coli*, mammalian cells and mice. *Dis. Model. Mech.* **2**, 508–515 (2009).
20. Fire, A. et al. Potent and specific genetic interference by double-stranded RNA in *Caenorhabditis elegans*. *Nature* **391**, 806–811 (1998).
21. Doudna, J. A. & Charpentier, E. The new frontier of genome engineering with CRISPR-Cas9. *Science* **346**, 1258096 (2014).
22. Percie Du Sert, N. et al. The ARRIVE guidelines 2.0: updated guidelines for reporting animal research. *BMJ Open Sci.* **4**, e100115 (2020).
23. Islam, Md. R. et al. The newt reprograms mature RPE cells into a unique multipotent state for retinal regeneration. *Sci. Rep.* **4**, 6043 (2014).
24. Casco-Robles, M. M., Yamada, S., Miura, T. & Chiba, C. Simple and efficient transgenesis with *I-SceI* meganuclease in the newt, *Cynops pyrrhogaster*. *Dev. Dyn.* **239**, 3275–3284 (2010).
25. Tanaka, H. V. et al. A developmentally regulated switch from stem cells to dedifferentiation for limb muscle regeneration in newts. *Nat. Commun.* **7**, 11069 (2016).
26. Casco-Robles, M. M. et al. Turning the fate of reprogramming cells from retinal disorder to regeneration by Pax6 in newts. *Sci. Rep.* **6**, 33761 (2016).
27. Konno, K., Yamasaki, M., Miyazaki, T. & Watanabe, M. Glyoxal fixation: An approach to solve immunohistochemical problem in neuroscience research. *Sci. Adv.* **9**, eadf7084 (2023).
28. Richter, K. N. et al. Glyoxal as an alternative fixative to formaldehyde in immunostaining and super-resolution microscopy. *EMBO J.* **37**, 139–159 (2018).

Acknowledgements

We thank Dr. Kuniharu Tasaki, Dr. Yuichi Kaji, and Dr. Sujin Hoshi (Institute of Medicine, University of Tsukuba) for their daily maintenance of mice as well as the administration and preparation of anesthetics. We express our gratitude to all members of the Japan Newt Research Community (JNRC) and the Newt Organ Regeneration Forum for their valuable comments and discussion. We also thank the citizens of Toride City for their assistance with the daily maintenance of Toride-Imori in the Imori-no-Sato field. This research was supported by the TMRC Collaborative Research Program (TB22-04; TB23-01) and the Japan Society for the Promotion of Science (24240062; 18H04061; 23H05483) to C.C.

Author contributions

C.C. and M.M.C.-R. conceived the idea and evaluated the data. M.M.C.-R. and C.C. designed and performed all experiments, and co-wrote the paper. S.M. and S.T. contributed to CRISPR-Cas9 KI mouse production. M.M.C.-R., Y.M., and M.H. contributed to wild-type and KI mice and evaluated the data. T.E. and T.S. contributed to the initial screening of the TA/AT-repeat-rich region in $\Delta CarA$. C.C., M.M.C.-R., and F.M. contributed to wild-type and transgenic newts and evaluated the data.

Competing interests

The authors declare the following competing interests. Patent applicant: UNIVERSITY OF TSUKUBA, Tsukuba, Japan. Name of inventor(s): CHIBA Chikafumi and CASCO ROBLES Martin Miguel. Title: NUCLEIC ACID FOR GENE EXPRESSION USES, GENE EXPRESSION VECTOR, METHOD FOR PRODUCING GENE EXPRESSION VECTOR, AND GENE EXPRESSION METHOD. Application number: PCT/JP2023/038909. Status of application: Published. Publication number: WO2024/090563. Publication date: 02 May 2024 (02.05.2024). All other authors declare no competing interests.

Additional information

Supplementary information The online version contains supplementary material available at <https://doi.org/10.1038/s42003-025-07759-9>.

Correspondence and requests for materials should be addressed to Martin Miguel Casco-Robles or Chikafumi Chiba.

Peer review information *Communications Biology* thanks Channabasavaiah Gurumurthy, Monica Sentmanat, and the other, anonymous, reviewer(s) for their contribution to the peer review of this work. Primary Handling Editors: Nishith Gupta and Rosie Bunton-Stasyshyn. A peer review file is available.

Reprints and permissions information is available at <http://www.nature.com/reprints>

Publisher's note Springer Nature remains neutral with regard to jurisdictional claims in published maps and institutional affiliations.

Open Access This article is licensed under a Creative Commons Attribution-NonCommercial-NoDerivatives 4.0 International License, which permits any non-commercial use, sharing, distribution and reproduction in any medium or format, as long as you give appropriate credit to the original author(s) and the source, provide a link to the Creative Commons licence, and indicate if you modified the licensed material. You do not have permission under this licence to share adapted material derived from this article or parts of it. The images or other third party material in this article are included in the article's Creative Commons licence, unless indicated otherwise in a credit line to the material. If material is not included in the article's Creative Commons licence and your intended use is not permitted by statutory regulation or exceeds the permitted use, you will need to obtain permission directly from the copyright holder. To view a copy of this licence, visit <http://creativecommons.org/licenses/by-nc-nd/4.0/>.

© The Author(s) 2025